Numerical Simulation Based Physical Parameter Analysis of Perovskite/c-Si Tandem PV Cells

Ahmad Halal[1], Ahmed Issa Alnahhal[1,2] and Balázs Plesz[1]
[1]Department of Electron Devices
Budapest University of Technology and Economics.
Budapest, Hungary

[2]Department of Biomedical Engineering
University of Palestine
Gaza Strip, Palestine

Abstract

In recent years, tandem solar cell technology (TSCs) has emerged as a great potential to overcome the efficiency limitations of single-junction solar cells by stacking two cells with different absorber materials with different bandgaps to absorb a broader wavelength range from the solar spectrum. Among different materials, Perovskite materials are considered as a promising candidate to be utilized in the top subcell of the tandem cell structure due to their tuneable bandgap, high absorption coefficient, and high carrier mobility. These advantages and the high flexibility of the upper perovskite cell (1.55-2 eV) make it compatible to be paired with the traditional c-Si (1.12 eV) as a tandem device. Optimally tailored matching between the two sub-cells of the tandem device will allow achieving high-performance TSCs. Thus, in this work, 2-terminal monolithic tandem cell-based on $CH_3NH_3PbI_3$ perovskite and c-Si is simulated using SCAPS-1D software. We investigated the thickness adjustment and doping concentration effect of the perovskite active layer with a particular focus on the effect of using different silicon wafer types (n- and p-type). The results showed a significant enhancement on tandem PV cell performance when we raise the doping concentration of the perovskite layer. It was found that a tandem cell constructed with a p-type silicon bottom cell exhibits higher PCE compared to that one constructed from n-type silicon. Overall, under a maximum total defect density of (10^{14} cm^{-3}), the configuration tandem cell of perovskite on Si-based p-type perovskite top cell with n-type bottom absorber layer cell demonstrated a J_{SC} of 17.63 mA/cm^2, V_{OC} of 1.861 V, FF of 73.57%, and a PCE of 24.13% under an optimum top layer thickness of 90.5 nm. While in the case of the p-Si bottom cell, the obtained efficiency is 28.31% with V_{OC} of 1.997 V, J_{SC} of 18.9 mA/cm^2, and FF of 75% under top layer thickness of around 100.7 nm.

Keywords: Tandem Solar cells, Perovskite, Crystalline Silicon, Perovskites Doping, Homojunction.

INTRODUCTION

Energy generation is essential for global expansion and is unquestionably the primary engine of economic development in the developing nations. Therefore, the increasing demand for energy consumption represents one of the most interesting challenges in the upcoming years. The necessity for alternative energy sources and the exploration of renewable energy sources has arisen in the last few decades with the decline in the use of traditional fossil fuel resources due to environmental issues and climate change problems. Among different renewable energy sources, solar cells continue to be one of the significant sources of energy in this respect [1]. Numerous PV systems have been developed to convert solar energy to electrical energy. Photovoltaic devices made of crystalline Si cover nearly 90% of the PV market with a record efficiency of 26.7% [2], the technology comes close to its theoretical maximum efficiency of 29.8% [3]. All other single junction cells (GaAs, perovskite, CIGS, etc.) are also subject to this limitation which means that there is only a little space for further development in the efficiency of single-junction solar cells. Therefore, the single junction devices are not sufficient for producing a high output power due to the fact that only a fraction of the solar energy can be converted by the cell due to high absorption loss and thermalization loss [4].

In recent years, multi-junction or tandem structures technology has emerged with a great potential to overcome this challenge and avail high efficiency that exceeds the Shockley-Queisser limit of single-junction solar cells by combining multiple absorption layers with materials having different bandgap energies. The upper sub-cell layer consists of a material with a wide bandgap constructed over a narrow bandgap material lower cell.

This configuration allows for absorbing a wide range of the solar spectrum, and it is capable of reducing the below band gap loss in addition to diminishing the thermalization loss. Bremner predicted that the conversion efficiency of multigap systems could be greater than 40% [5]. However, although tandem structures are more efficient, manufacturing costs and complexity make them more expensive. Therefore, creating a cost-effective tandem becomes an interesting goal for researchers [6].

Targeting commercial applications, tandem cells based on c-Si bottom cells have been proposed and developed on a low-cost Si substrate [7] for the purpose of producing high-efficiency and low-cost PV modules. However, a major drawback of this technique has been the lack of materials with a high open-circuit voltage (V_{OC}) that are within the requisite bandgap range of 1.55 to 1.9 eV for use in the upper cell of the tandem configuration [8]. The development of methyl-ammonium-lead-halide perovskite over the past years has considerably influenced this issue and opened the path to utilize it as the top cell in Si-based tandem cells, thanks to its features such as high absorption coefficient, high charge carrier mobilities and diffusion lengths. This material exhibits not only a significant efficiency and high open-circuit voltages (V_{OC}) but also low processing cost. Furthermore, perovskite materials have a bandgap of 1.5-2 eV, allowing them to be a good absorbent material in the ultraviolet and visible light ranges and completely transparent in the infrared region. This bandgap can be precisely tuned to greater values by adding Br or Cl, making them able to reach 1.75 eV, which is considered the optimum bandgap for use in the top cell designing of highly efficient crystalline silicon (c-Si)-based tandem solar cells [9].

Perovskite/crystalline silicon tandem cells can be implemented in different architectures according to their fabrication methods and electrical connection [9]. They can either be designed as an electrically separated cell and coupled by optical filters called 4-terminal or can be as a monolithic device called 2-terminal configuration. The monolithic structure or two-terminal configuration contains fewer functional layers resulting in the potential low processing steps and low electrical and optical losses. In this design, perovskite/crystalline silicon tandem cells are considered to be a single unit in which both the top and bottom sub-cells are electrically connected in series through a recombination layer and the total V_{OC} of the tandem is the summation of the two cell voltages. One limitation of this design is the current mismatch between the two sub-cells which will cause charge carrier accumulation at the recombination contact and affect the tandem device functionality. So, it is important to ensure current matching between the upper and lower tandem sub-cells when we are dealing with this tandem design.

Although the PCE of 2-terminal perovskite on c-Si tandem cells can exceed 30% [10], the highest current record is around 29.15% [11]. Therefore, a successful commercial entry is likely to require even greater values of PCE to compete with existing non-perovskite tandem technologies. Many prime parameters have an impact on the PCE improvement of 2-terminal perovskite on c-Si tandem cells and need to be investigated. One of the main parameters in this structure is the requirement of strict current matching between the two sub-cells to reach an optimal tandem efficiency. Other characteristics parameters such as the absorber layer thickness, defect density, and doping concentration need to be examined to understand the influence of these parameters on the performance of 2-terminal perovskite/c-Si tandem cells. Inspecting these parameters experimentally will require enormous resources in terms of time and material consumption. As a result, an appropriate simulation technique is required to assist optimization activities in a faster and more cost-effective manner.

The main goal of this study is to analyse and improve a 2-terminal configuration $MAPbI_3$-on-c-Si tandem devices through numerical simulation studies using the SCAPS-1D simulation tool to better understand the effect of varying different physics parameters characteristics on the performance of the perovskite/c-Si tandem device. Furthermore, our approach for this investigation involves addressing the following points:

- Establishment of the perovskite/c-Si tandem model.
- Validating the simulated results with data published for experimentally fabricated perovskite/c-Si of the same structure.
- Effect of the absorber layers defect density on tandem device performance.
- Effect of absorber layers doping concentration.
- Optimization of absorber layers thickness.
- Investigating the performance of tandem solar cells by inverting the upper cell structure and using opposite dopant type silicon wafer types.

The anticipated outcomes of this study will provide a valuable design guideline for high-performance, low-cost monolithic perovskite/c-Si tandem PVs.

METHODOLOGY

Solar cell devices could be simulated using any numerical software that can solve the basic semiconductor equations. Among different simulation software, SCAPS software has the ability to analyse heterojunction and multijunction solar configuration by varying up to 7 layers. Furthermore, the simulation results are in good agreement with experimental results. This one-dimensional simulation software was established and developed by ELIS, University of Gent, Belgium [12]. It is utilized in this work to numerically

predict the most suitable electronic, electrical and optical properties of the perovskite/c-Si tandem device.

Three basic semiconductor equations, namely, Poisson's (1), electron continuity equation (2), and hole continuity equation (3), are utilized by SCAPS software to compute several electrical and optical properties of the solar cell, such as energy bands, J-V characteristics curve, and spectral response (QE) curve. These curves are used to obtain V_{OC}, J_{SC}, fill factor and the conversion efficiency of the simulated device.

$$\frac{d}{dx}\left(-\epsilon(x)\frac{d\psi}{dx}\right) = q[p(x) - n(x) + N_D^+(x) - N_A^-(x) + p_t(x) - n_t(x)] \quad (1)$$

$$\frac{dp_n}{dt} = G_p - \frac{p_n - p_{n0}}{\tau_p} + p_n\mu_p\frac{d\zeta}{dx} + \mu_p\zeta\frac{dp_n}{dx} + D_p\frac{d^2p_n}{dx^2} \quad (2)$$

$$\frac{dn_p}{dt} = G_n - \frac{n_p - n_{p0}}{\tau_n} + n_p\mu_n\frac{d\zeta}{dx} + \mu_n\zeta\frac{dn_p}{dx} + D_n\frac{d^2n_p}{dx^2} \quad (3)$$

Where ϵ is the permittivity, ψ is the electrostatic potential, N_A^- and N_D^+ are the shallow acceptor and donor concentrations, q is the electron charge, $n_t(x)$ and $p_t(x)$ indicates the concentrations of trapped electrons and holes, G_p and G_n are the generation rate of holes and electrons, ζ is the electric field, μ_p and μ_n indicates the hole and electron mobilities, τ_p and τ_n are the lifetime of holes and electrons, D_p and D_n are the diffusion coefficients for hole and electron, respectively.

The following formula is used to determine the fill factor (FF) of the device:

$$FF = \frac{J_{MP}V_{MP}}{J_{SC}V_{OC}} \quad (4)$$

Here, V_{MP} and J_{MP} are the voltage and current density at the maximum power points. The tandem cell efficiency (η), normalized to input power (P_{in}), is defined as:

$$\eta = \frac{V_{OC}\,J_{SC}\,FF}{P_{in}} \quad (5)$$

The two sub-cells can be described as two diodes connected in series for the 2-terminal monolithic tandem cell. Therefore, the open-circuit voltage (V_{OC}) is the summation of both upper and lower cell voltages, while the short-circuit current density J_{SC} is determined by the minimum current supplied by the two sub-cells.

DEVICE STRUCTURE AND SIMULATION PARAMETERS

We have simulated a monolithic 2-terminal tandem structure according to the experimental design proposed in literature [13]. A conventional p-i-n configuration is used as a top cell. The top cell layers are Spiro-OMeTAD/Perovskite/TiO_2. Here, an intrinsic $MAPbI_3$ is used as a large bandgap absorbent layer of the upper cell sandwiched between p-type Spiro-OMeTAD acting as the hole transport layer (HTL) and n-type TiO_2 as the electron transport layer (ETL). Whereas the bottom cell layers consist of an n-type Si, which represents the lower bandgap absorbent layer, with p^{++} Si as an emitter layer and n^{++} Si as the back surface field layer. These two sub-cells are connected in series through a recombination junction. Fig. 1 illustrates the modelled tandem cell configuration designed in this work.

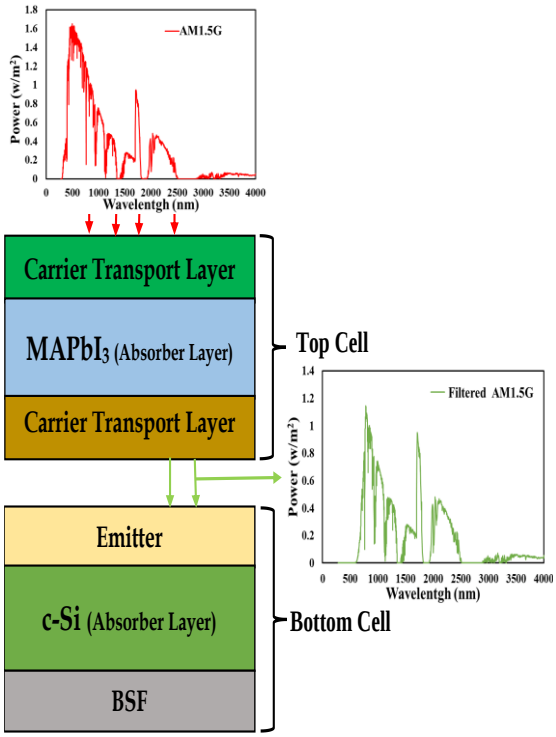

Fig.1. Tandem Cell Device Structure.

Photovoltaic device performance is highly dependent on the parameters such as layers thickness, charge carrier concentration, temperature, shunt and series resistances, and so on. The proposed tandem device is simulated under standard illumination condition of AM 1.5 G and a working temperature of 300 K. The basic physic parameters such as (materials bandgap, electron affinity, Dielectric constant, etc.) that are used for performing this simulation are adopted from the following published literature [14], [15], [16] as it is shown in Table 1. Other parameters such as doping concentration, layers thickness, etc. are adjusted to fit the performance of the simulated device to an experimentally fabricated one of the same structures [13].

It is worth mentioning that SCAPS does not fully support the simulation of multijunction solar cells since the optical coupling of the upper and lower cell is not considered. Therefore, to numerically analyze the tandem device using SCAPS-1D, a filtered spectrum has to be calculated in which the top sub-cell is exposed to the standard solar spectrum while the bottom cell will receive the transmitted spectrum from each layer of the top cell layers. This filtered spectrum is given by:

Parameters	Materials					
	Spiro-OMeTAD	***MAPbI₃***	***TiO₂***	***p⁺Si***	***nSi***	***n⁺Si***
Thickness (µm)	0.030	Variable	0.030	0.1	200	1
Dielectric constant	3	30	9	11.9	11.9	11.9
Electron affinity (eV)	2.45	3.9	4.26	4.05	4.05	4.05
Band gap (eV)	3	1.55	3.2	1.12	1.12	1.12
Effective conduction band density (cm^{-3})	2.2×10^{19}	1×10^{14}	3×10^{13}	2.819×10^{19}	2.819×10^{19}	2.819×10^{19}
Effective valence band density (cm^{-3})	1.8×10^{19}	1.8×10^{20}	1.8×10^{19}	1.04×10^{19}	1.04×10^{19}	1.04×10^{19}
Effective electron (hole) mobility (cm^2/Vs) Mn/Mp	$2\times10^{-4}/2\times10^{-4}$	50/50	20/10	1400/450	1400/450	1400/450
Doping concentration acceptors (cm^{-3})	2×10^{18}	0	0	1×10^{18}	0	0
Doping concentration donators (cm^{-3})	0	0	1×10^{16}	0	Variable	1×10^{18}
Electron thermal velocity (cm/s)	1×10^{7}	1×10^{7}	1×10^{7}	1×10^{7}	1×10^{7}	1×10^{7}
Hole thermal velocity (cm/s)	1×10^{7}	1×10^{7}	1×10^{7}	1×10^{7}	1×10^{7}	1×10^{7}
Bulk defect type	Neutral	Neutral	Neutral	Neutral	Neutral	Neutral
Bulk defect (cm^{-3})	Variable	Variable	Variable	Variable	Variable	Variable
Capture cross section electrons (cm^{-2})	1×10^{-15}	1×10^{-15}	1×10^{-15}	1×10^{-15}	1×10^{-15}	1×10^{-15}
Capture cross section holes (cm^{-2})	1×10^{-15}	1×10^{-15}	1×10^{-15}	1×10^{-15}	1×10^{-15}	1×10^{-15}

Table 1: Input parameters for SCAPS-1D simulation software [14], [15], [16].

$$S(\lambda) = S_0(\lambda).exp\left(\sum_{i=1}^{3} -\left(\alpha_{material_i}(\lambda).d_{material_i}\right)\right) \quad (6)$$

Where $S(\lambda)$ is the transmitted light from the upper cell, $S_0(\lambda)$ is the standard incident spectrum (AM 1.5G) on the upper cell, α is the absorption coefficient, and d represents the thickness of the respective layer. The reflection losses from each interface are ignored. We have assumed a Gaussian defect energy level of 0.6 eV below the conduction band with a characteristic energy of 0.1 eV for both of the two sub-cells [14,16]. The extracted value of shunt resistance in this work is infinity, while the series resistance is set to be 7.5 Ω.cm^2. These values gave the best fitted J-V curve to the experimental one.

RESULTS AND DISCUSSIONS

Validation of existing perovskite/c-Si tandem solar cell

The base tandem solar cell model "Spiro-OMeTAD/ Perovskite/ TiO_2/ p^{++}-Si/ n^+-Si/ n^{++}-Si" was simulated in SCAPS-1D to be validated on an existing perovskite/c-Si tandem device from literature. Fig. 2 shows the J-V curve comparison of the tandem cell structure simulated in SCAPS-1D in comparison with the experimental one adopted from the literature [13]. The simulation results of the designed tandem model reveal a J_{SC} of 11.58 mA/cm^2 and V_{OC} of 1.57 V with an FF and efficiency values of 74% and 13.5%, respectively. These simulation results fit well to the reported work, indicating the built model is suitable for describing the given solar cell structure.

The short-circuit current density J_{SC} of perovskite and c-Si sub-cells are 11.55 mA/cm^2 and 14.7 mA/cm^2, respectively. These J_{SC} values of the two sub-cells also match the reported work in the literature. However, it is clearly noticeable from these results that this reported structure is suffering losses due to the unbalanced current matching between the two sub-cells, and the total short-circuit current density of the tandem cell is limited by the perovskite top cell current. The small short-circuit current density J_{SC} of the perovskite sub-cell is due to the thinner layer that had been used in the tandem structure, while in the case of c-Si, a high level of defect density leads to the limitation of the J_{SC} of this bottom cell. The effects of these parameters on the reported work and the optimization steps for the present work will be discussed in detail in the following sections.

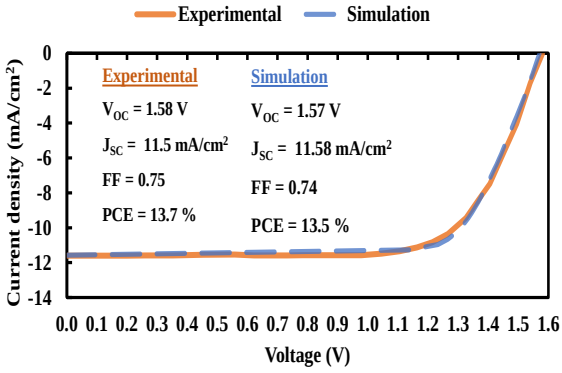

Fig.2. Published experimental curves [13] and simulated J-V curves of the perovskite on Si-based tandem PV cell.

Defect density effect on the tandem solar cell performance.

The performance of solar cells is significantly influenced by the quality of the absorber layers. A high level of defect density in the different absorber layers of tandem configuration will lead to a high recombination rate which in turn will exterminate the charge carriers and degrade device performance. Thus, the defect density value was varied, and the J-V characteristics were determined. The results are shown in Fig. 3.

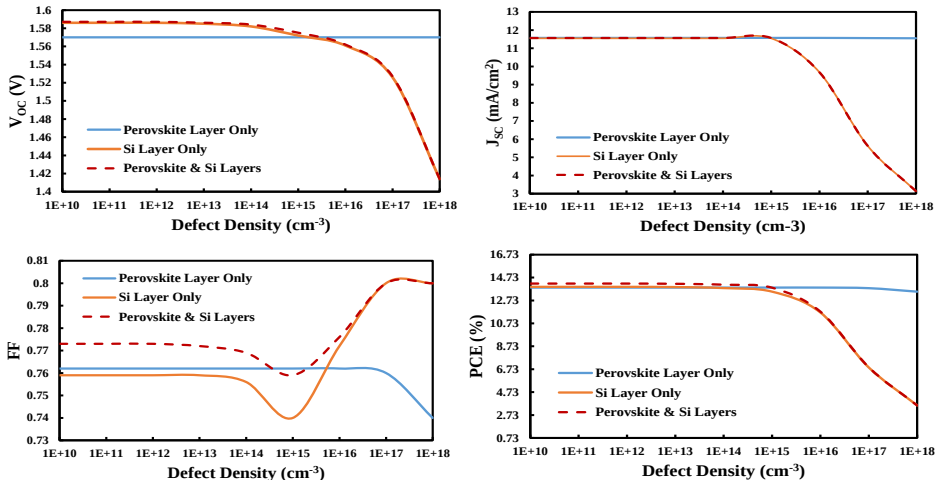

Fig.3. Electrical performance characteristics of perovskite/c-Si tandem cell under the effect of different defect density.

It can be seen clearly in Fig. 3. that this tandem PV device is susceptible to the defects in the Si absorber layer while increasing the defect density in the perovskite absorber layer even to a higher level will not have a significant effect on the performance of the tandem device. This is mainly due to the thicker Si layer used in the bottom cell compared to the thinner perovskite layer of the tandem design. Therefore, to achieve high efficiency of the perovskite/c-Si tandem solar cell, it is essential to fabricate a high-quality crystalline silicon PV cell which will be utilized in the bottom cell of the tandem design. For the optimization process in this paper, the defect density was kept as low as possible and values of 1×10^{14} cm^{-3} and 1×10^{13} cm^{-3} were chosen for the rest of the work as the defect density in the absorbent layers of $MAPbI_3$ and c-Si, respectively.

Doping concentration effect on the tandem solar cell performance.

The doping density in the absorber layer has a prominent influence on PV solar cell performance.

According to the experimental reported work, an n-type Si wafer is used as the base layer of the tandem bottom cell. Therefore, we varied the donor concentration of this layer from 10^{15} to 10^{21} cm^{-3} to examine the effect of increasing the doping concentration on the tandem PV cell's overall performance. In addition to that, we investigated the influence of doping the intrinsic layer of the perovskite absorber layer by increasing the acceptor concentration up to 10^{21} cm^{-3} to form a p-type $MAPbI_3$. Thus, in the upcoming optimization steps, we are going to use a p-p-n configuration in the top sub-cell of the tandem device instead of p-i-n, which was used in the reported work. The term structure A will be used to describe this configuration of the tandem device. However, p-type $MAPbI_3$ was formed in this work instead of n-type $MAPbI_3$ because n-type $MAPbI_3$ is more difficult to realize due to the formation of neutral defects or compensation from intrinsic point defects [17].

According to Fig. 4, raising the doping concentration of the perovskite layer has a significant influence on tandem

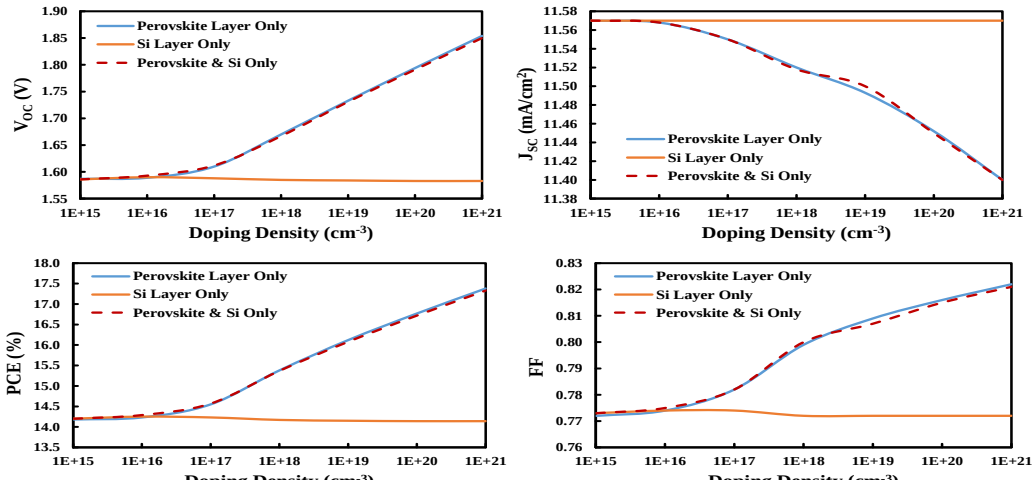

Fig.4. Electrical performance characteristics of perovskite/c-Si tandem cell under the effect of different doping concentration.

PV cell performance enhancement, but excessive doping of the Si layer has a negative impact on tandem device performance. Although there was a slight decrease in short-circuit current, the tandem device efficiency increased dramatically as the perovskite layer doping concentration was increased. This was due to the increase in open-circuit voltage that occurred due to the increase in perovskite layer doping concentration. However, PCE is maximized at $N_A = 1\times10^{21}$ cm^{-3} and $N_d = 1\times10^{17}$ cm^{-3} for $MAPbI_3$ and c-Si, respectively. Therefore, these doping values will be used in the rest of the work in this paper.

Optimization of the thickness of the tandem sub-cells

In 2-terminal monolithic tandem configurations, Adjusting the current between the two sub-cells is extremely important because the current mismatch will cause charge carriers to accumulate at the recombination contact, which affects the recombination behaviour negatively. As previously stated, the fabricated structure referenced from literature lacks a well-balanced current matching between the two sub-cells and thus the total short-circuit current density of the tandem cell is restricted by the perovskite top cell's current. In the previous sections the defect density and doping concentration have been optimized. As a next step the thickness of the absorber layers will be optimized to accomplish a good current matching between the two sub-cells. This is done by increasing the thickness of the simulated perovskite layer to match the same J_{MPP} or J_{SC} values for both sub-cells. To reach the best current matching condition, the top cell thickness is varied from 75 nm to 95 nm. However, the best matching between the two sub-cells short circuit-currents J_{SC} is achieved with 90.5 nm top cell thickness, where the top and bottom cells produce J_{SC} of 17.63 mA/cm^2 and 17.63 mA/cm^2, respectively, as illustrated in Fig. 5.

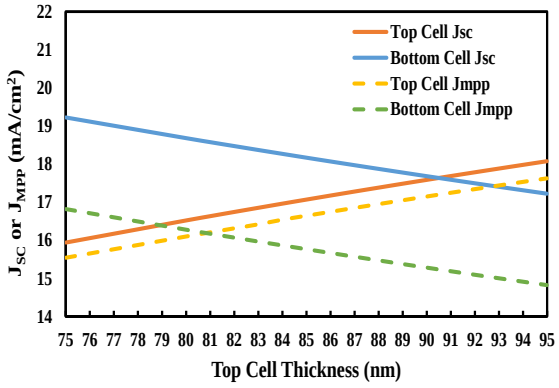

Fig.5. J_{SC} and J_{MPP} comparisons between the top and bottom sub-cells of structure A.

At this match current point and due to the previous optimization processes of defect density and doping concentration, the perovskite/c-Si solar cell efficiency is reached 24.13% from comprising 18.95% perovskite of p-n-n configuration as a top cell and 9.24% c-Si of p-n structure as a bottom cell. The optimized perovskite/c-Si PV device exhibited a fill factor of 73.57%, with J_{SC} and V_{OC} of 17.63 mA/cm^2 and 1.861 V, respectively. The J-V curve is illustrated in Fig. 6.

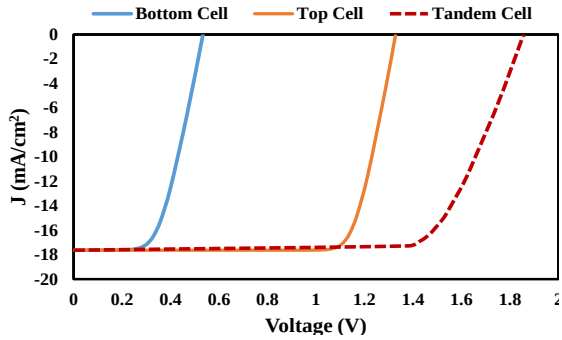

Fig.6. J-V curves of the optimized Structure A.

The effect of the c-Si doping type in the bottom cell of the tandem structure.

We investigated the effect of the doping type of the c-Si bottom cell's base layer on the tandem solar cell performance. We replaced the bottom cell layers of the reported work by considering a p-type c-Si as the base layer together with n^{++} Si as an emitter layer and p^{++} Si as the back surface field layer. The layer stacking order of the perovskite top cell is adjusted to a n-p-p configuration of TiO_2/p-type-perovskite/Spiro-OMeTAD. The term structure B will be used to describe this modified configuration of the tandem device. The optimization steps for defect density and doping density are applied again to the modified structure of the perovskite on the c-Si tandem device. It is found that PCE is maximized at the same previous values of doping concentration and defect density that have been used previously to optimize the reported work. The current matching condition between the two sub-cells is achieved by varying the absorber layer thickness of the perovskite top cell from 90 to105 nm to match the same J_{MPP} or J_{SC} values for both sub-cells. However, the matching point between the two sub-cells short-circuit current J_{SC} is acquired with 100.7 nm of the perovskite absorber layer thickness, where the top and bottom sub-cells produce J_{SC} of 18.9 mA/cm^2 and 18.9 mA/cm^2, respectively as shown in Fig. 7.

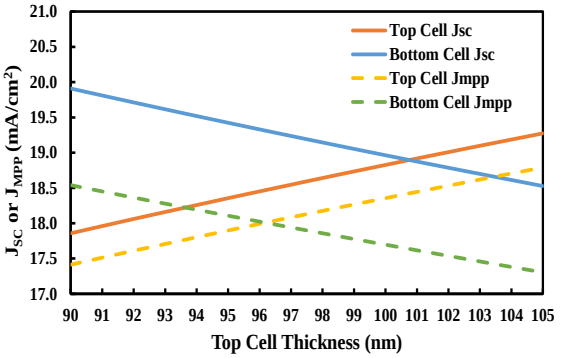

Fig.7. J_{SC} and J_{MPP} comparisons between the top and bottom sub-cells of structure B.

Using an absorber layer of p-type c-Si instead of n-type c-Si led to a significant enhancement in the performance of the tandem device. This modified structure (structure B) exhibits an efficiency of 28.31% compared to the 24.13% of the previous optimized design (structure A) and the 13.7 % of the reported experimental work. The J-V characteristics of the perovskite/c-Si tandem cell are illustrated in Fig. 8. The high output results of this structure can be attributed to the fact that in the p-type c-Si absorber layer, the minority charge carriers are the electrons which have a higher diffusion length and a higher probability of reaching the junction without recombining and hence getting separated than holes. Therefore, it is essential to construct the base layer of the bottom cell of the perovskite/c-Si tandem cell with a p-type semiconductor because it has electrons as minority charge carriers.

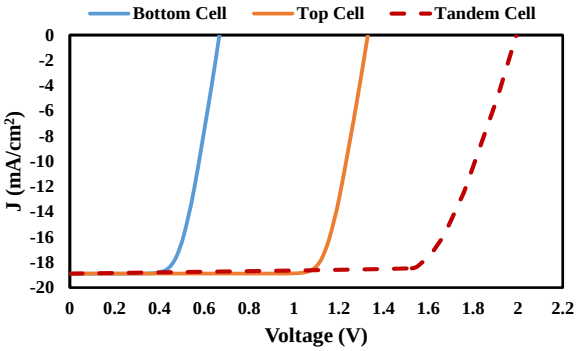

Fig.8. J-V curves of the optimized Structure B.

The electrical performance characteristics of the reported work and the two optimized structures are summarized in Table 2.

Structures / Parameters	Reported Work [13]			Optimized Structure A			Optimized Structure B		
	Top Cell	*Bottom Cell*	*Tandem Cell*	*Top Cell*	*Bottom Cell*	*Tandem Cell*	*Top Cell*	*Bottom Cell*	*Tandem Cell*
J_{SC} (mA/cm^2)	11.5	14.7	11.5	17.63	17.63	17.63	18.9	18.9	18.9
V_{OC} (V)	-	-	1.58	1.328	0.533	1.861	1.33	0.667	1.997
V_{MPP} (V)	-	-	-	1.102	0.358	1.426	1.095	0.472	1.568
J_{MPP} (mA/cm^2)	-	-	-	17.196	15.232	16.92	18.417	17.639	18.055
FF (%)	-	-	75	80.91	58	73.57	80.24	66.12	75
PCE (%)	-	-	13.7	18.95	9.24	24.13	20.16	14.62	28.31

Table 2: Electrical characteristics of the reported work and the two optimized perovskite/c-Si tandem structures.

CONCLUSION

A numerical simulation for perovskite/c-Si monolithic tandem solar cells was performed using SCAPS-1D. After validating our model with experimental results from the literature, our achieved results have enabled us to select the best parameters, such as optimal doping concentration, defect density, and thickness of the perovskite top cell that leading to the highest possible efficiencies. We found that perovskite silicon-based tandem solar cell performance is less sensitive to the defect density of the perovskite absorber layer than the defect density of the c-Si base layer. In addition, utilizing highly doped p-type $MAPbI_3$ instead of the intrinsic perovskite could have a significant effect on the enhancement of the tandem cell output results. At the same time, it is essential to use a moderate doping concentration in the base layer of the c-Si bottom cell. This structure demonstrated an efficiency of 24.13% with a J_{SC} of 17.63 mA/cm^2, V_{OC} of 1.861 V, and FF of 73.57%, under an optimum top absorber layer thickness of 90.5 nm. Moreover, we found that using p-type c-Si instead of n-type c-Si as the base layer of the bottom cell could increase device efficiency further, enabling a PCE of 28.31% with FF of 75% and 18.9 mA/cm^2 and 1.997 V of short-circuit current and open-circuit voltage, respectively, under top layer thickness of around 100.7 nm.

Overall, the presented results in this study demonstrate a beneficial guideline for designing an optimal perovskite on Si tandem solar cells, which can open the path toward the development of high-efficiency and low-cost tandem solar cells in the future.

ACKNOWLEDGEMENTS

The research reported in this paper and carried out at Budapest University of Technology and Economics was partially supported by the Stipendium Hungaricum Scholarship Program of the Hungarian Government and the project number 2020-1.1.2-PIACI-KFI-2021-00242 of the National Research, Development and Innovation Office (NKFIH).

REFERENCES

[1] Kannan, N. and Vakeesan, D.: Solar energy for future world:-A review, Renewable and Sustainable Energy Reviews **62**, 2016, 1092-1105.

[2] Yoshikawa, K., Kawasaki, H., Yoshida, W., Irie, T., Konishi, K., Nakano, K., Uto, T., Adachi, D., Kanematsu, M., Uzu, H. and Yamamoto, K.: Silicon heterojunction solar cell with interdigitated back contacts for a photoconversion efficiency over 26%, Nature energy, **2(5)**, 2017, 1-8.

[3] Swanson, R.M., et al: Approaching the 29% limit efficiency of silicon solar cells, In Conference Record of the Thirty-first IEEE Photovoltaic Specialists Conference (Lake Buena Vista, 2005), 889–894.
[4] Shockley, W. and Queisser, H.J.: Detailed balance limit of efficiency of p-n junction solar cells, Journal of applied physics, **32(3)**, 1961, 510–519.
[5] Bremner, S.P., Levy, M.Y. and Honsberg, C.B.: Analysis of tandem solar cell efficiencies under AM1. 5G spectrum using a rapid flux calculation method, Progress in photovoltaics: Research and Applications, **16(3)**, 2008, 225-233.
[6] Choi, W., Kim, C.Z., Kim, C.S., Heo, W., Joo, T., Ryu, S.Y., Kim, H., Kim, H., Kang, H.K. and Jo, S.: A repeatable epitaxial lift-off process from a single GaAs substrate for low-cost and high-efficiency III-V solar cells, Advanced Energy Materials, **4(16)**, 2014, 1400589.
[7] Mailoa, J.P., Bailie, C.D., Johlin, E.C., Hoke, E.T., Akey, A.J., Nguyen, W.H., McGehee, M.D. and Buonassisi, T.: A 2-terminal perovskite/silicon multijunction solar cell enabled by a silicon tunnel junction, Applied Physics Letters, **106(12)**, 2015, 121105.
[8] Meillaud, F., Shah, A., Droz, C., Vallat-Sauvain, E. and Miazza, C.: Efficiency limits for single-junction and tandem solar cells, Solar energy materials and solar cells, **90(18-19)**, 2006, 2952-2959.
[9] Werner, J., Niesen, B. and Ballif, C.: Marriage of convenience or true love story?–An overview, Advanced Materials Interfaces, **5(1)**, 2018, 1700731.
[10] Filipič, M., Löper, P., Niesen, B., De Wolf, S., Krč, J., Ballif, C. and Topič, M.: CH 3 NH 3 PbI 3 perovskite/silicon tandem solar cells: characterization based optical simulations, Optics express, **23(7)**, 2015, A263-A278.
[11] Al-Ashouri, A., Köhnen, E., Li, B., Magomedov, A., Hempel, H., Caprioglio, P., Márquez, J.A., Morales Vilches, A.B., Kasparavicius, E., Smith, J.A. and Phung, N.: Monolithic perovskite/silicon tandem solar cell with> 29% efficiency by enhanced hole extraction. Science, **370(6522)**, 2020, 1300-1309.
[12] M. Burgelman, K. Decock, A. Niemegeers, J. Verschraegen, and S. Degrave: *Scaps manual*, 2016.
[13] Mailoa, J.P., Bailie, C.D., Johlin, E.C., Hoke, E.T., Akey, A.J., Nguyen, W.H., McGehee, M.D. and Buonassisi, T.: A 2-terminal perovskite/silicon multijunction solar cell enabled by a silicon tunnel junction, Applied Physics Letters, **106(12)**, 2015, 121105.
[14] Minemoto, T. and Murata, M.: Theoretical analysis on effect of band offsets in perovskite solar cells, Solar Energy Materials and Solar Cells, **133**, 2015, 8-14.
[15] Löper, P., Stuckelberger, M., Niesen, B., Werner, J., Filipic, M., Moon, S.J., Yum, J.H., Topič, M., De Wolf, S. and Ballif, C.: Complex refractive index spectra of CH3NH3PbI3 perovskite thin films determined by spectroscopic ellipsometry and spectrophotometry, The journal of physical chemistry letters, **6(1)**, 2015, 66-71.
[16] Kim, K., Gwak, J., Ahn, S.K., Eo, Y.J., Park, J.H., Cho, J.S., Kang, M.G., Song, H.E. and Yun, J.H.: Simulations of chalcopyrite/c-Si tandem cells using SCAPS-1D, Solar Energy, **145**, 2017, 52-58.
[17] Shi, T., Yin, W.J. and Yan, Y.: Predictions for p-type CH3NH3PbI3 perovskites, The Journal of Physical Chemistry C, **118(44)**, 2014, 25350-25354.

Addresses of the authors

Ahmad Halal, 1117 Budapest, Magyar tudósok krt. 2, Budapest, Hungary, ahmadhalalftesah@edu.bme.hu
Ahmed Issa Alnahhal, 1117 Budapest, Magyar tudósok krt. 2, Budapest, Hungary, aalnahhal@edu.bme.hu
Balázs Plesz, 1117 Budapest, Magyar tudósok krt. 2, Budapest, Hungary, plesz.balazs@vik.bme.hu